J Therm Anal Calorim (2010) 101:119–127
DOI 10.1007/s10973-009-0542-1

Calorimetric study of ternary binder of calcium aluminate cement, Portland-limestone cement and FGD gypsum

Wenbin Lou · Baohong Guan · Zhongbiao Wu

Received: 9 July 2009 / Accepted: 2 October 2009 / Published online: 4 November 2009

Abstract To use flue gas desulfurization (FGD) gypsum and limestone as supplement of cement, conduction calorimetry was applied to investigate the early hydration of ternary binder of calcium aluminate cement (CAC), Portland-limestone cement (PLC), and FGD gypsum, supplemented with the determination of setting times and X-ray diffraction (XRD) analysis. Different exothermal profiles were presented in two groups of pastes, in which one group (group A) sets the mass ratio of FGD gypsum/CAC at 0.25 and the other group (group B) sets the mass ratio of PLC/CAC at 0.25. Besides the two common exothermal peaks in cement hydration, a third exothermal peak appears in the pastes with 5–15% FGD gypsum after gypsum is depleted. It is found that not PLC but FGD gypsum plays the key role in such ternary binder where the reaction of ettringite formation dominates the hydration process. PLC accelerates the hydration of ternary binder, which mainly attributes to the nucleating effect of fine limestone particles and PC clinker. The modified hydration process and mechanism in this case is well visualized by the means of calorimetry and it helps us to optimize such design of ternary cementitious material.

Keywords Calcium aluminate cement · Calorimetry · FGD gypsum · Hydration · Portland-limestone cement

W. Lou · B. Guan (✉) · Z. Wu
Department of Environmental Engineering, Zhejiang University, 310027 Hangzhou, China
e-mail: guanbaohong@zju.edu.cn

Introduction

Flue gas desulfurization (FGD) gypsum is a by-product generated from lime-gypsum wet flue gas desulfurization, which is the most common technology for SO_2 emission control in coal-fired power plants. FGD gypsum is mainly composed of calcium sulfate dihydrate and has been widely applied in plasterboard manufacture and Portland cement (PC) production as raw material instead of nature gypsum [1]. However, these uses of FGD gypsum are insufficient considering the huge amount of its production, and it is mainly ascribed to technology limit. For example, only about 3–5% FGD gypsum is suitable for being mixed in the clinker in PC production [2, 3]. So it is eager to explore other effective ways to utilize the continuous increasing output of FGD gypsum, and the ettringite ($3CaO{\cdot}Al_2O_3{\cdot}3CaSO_4{\cdot}32H_2O$, AFt) based material could bring us prospect.

A vivid example of ettringite-based material is calcium sulfoaluminate (CSA) cement, which has replaced PC in some application fields. Its versatile applications in development of concrete with high early strength, self-leveling screed with limited curling and glass-fiber-reinforced cement have been exhibited [4, 5]. Similar performance could be achieved in a binary composition of calcium aluminate cement (CAC) and gypsum [6], where monocalcium aluminate (CA, notation commonly used in cement chemistry: C=CaO, A=Al_2O_3, H=H_2O, S=SiO_2, $\hat{S}$=SO_3), the main mineral phase in CAC and gypsum react with water as the following Eq. 1 shows:

$$3CA + 3C\hat{S}H_2 + 32H \rightarrow C_6A\hat{S}_3H_{32} + 2AH_3 \quad (1)$$

Consequently, ettringite and AH_3 gel are generated. When lime exists, Eq.1 is substituted by reaction Eq. 2.

$$3CA + 9C\hat{S}H_2 + 72H + 6CH \rightarrow 3C_6A\hat{S}_3H_{32} \quad (2)$$

Thus, more FGD gypsum could react with CAC clinker, which means more consumption of gypsum and economical beneficial.

However, it should be noted that characteristic of ettringite in these cementitious materials is strongly dependent on whether lime exists. PC is saturated in lime solution during its hydration, and the ettringite formed under such condition is expansive [7]. Ettringite formed in the absence of lime is less or no expansive and generates high early strength [7, 8]. The failures in the ternary cementitious composition of CAC/PC/gypsum are usually caused by a large amount of expansive ettringite [9]. It indicates that the amount of PC clinker is crucial to the performance of such ternary cementitious materials.

As far as economical and environmental benefits are concerned, limestone has been widely investigated as an important supplement in composite cement. In fact, Portland-limestone cements (PLCs) are the most widely used cements in Europe. The European Standard EN197-1 identifies two PLCs, CEM II/A-L and CEM II/B-L, in which the maximum contents of limestone are 20 and 35%, respectively [10]. In China, the Standard of Construction Material (JC 600-2002) was published in 2002 using the EN197-1 as a template.

A lot of studies have focused on the performance of PLC and the effects of limestone on cement hydration, and the general accepted view is that limestone can accelerate the hydration of PC by nucleating effect of introduced fine particles [11–13]. The influence of limestone on CAC hydration has also been investigated and the similar mechanism is found [14, 15]. However, no work has been dealt with the influence of limestone on hydration of ternary cementitious material of CAC, PLC, and gypsum.

Isothermal calorimetry has shown its versatility in studying the hydration kinetics of cementitious systems and help to screen cement-admixture combinations with respect to hydration stability [16, 17]. During last decades, this method has been used to study a variety of cementitous systems, for example, PC mixed with fly ash [18, 19], silica fume [20], metakaolins [21], combustion by-products [22], and limestone [12, 13]; CAC blended with refractory corundum [23] and limestone [14]; mixes of PC and high alumina cement [16, 24].

In authors' previous work, the hydration behavior of CAC blended with FGD gypsum was revealed [25]. Here, a further-step experimental work of calorimetry is presented with the aim of better understanding the hydration process and mechanism involved in ternary binder of CAC, PLC, and FGD gypsum. The attention is focused on limestone and PC clinker influence on the hydration. The study follows by other standard measurements, helps us to optimize such ternary cementitious material design and to elucidate the scale of FGD gypsum utilization in cement, an important task from by-product utilization point of view.

Experimental

Materials

FGD gypsum is from Ban Shan Power Plant, Hangzhou, China. Its main chemical compositions are given in Table 1 and the mineral phases are further confirmed by XRD analysis (Fig. 1). The mass percentage of calcium sulfate dihydrate is up to 94.3% and the main impurities are quartz and limestone. Some harmful impurities such as B, Pb, Ni, Cr, As, Cd, and Hg, have also been measured but not present in Table 1 for their extremely low contents.

The chemical compositions of a commercial calcium aluminate cement CAC-50, in which the Al_2O_3 mass percent is between 50 and 60% according to the China National Standard: GB 201-2000, are also shown in Table 1. XRD patterns (Fig. 1) indicate that gehlenite (C_2AS) rather than CA is the major mineral. To avoid negative effect of excessive PC clinker and to intensify the effect of limestone on hydration, the PLC used here is not a commercial product but a mixture with 25% PC clinker and 75% limestone. The chemical compositions of PLC are also shown in Table 1. XRD patterns (Fig. 1) point out the mineral of Alite (C_3S) and Belite (β-C_2S) from PC clinker, calcite and dolomite from limestone.

Figure 2 shows the particle size distributions of three raw materials. The FGD gypsum is not ground and it is quite coarse. Its main particles distribute narrowly between 10 and 100 μm with the mean particle size of 52.2 μm. CAC and PLC exhibit the similar particle size distribution,

Table 1 Chemical compositions of FGD gypsum, CAC, and PLC

Oxides/elements	Chemical compositions/wt%		
	FGD gypsum	CAC	PLC
CaO	31.76	34.0	55.80
SO_3	43.87	–	0.13
SiO_2	2.00	8.0	5.10
CO_2	0.82	–	33.0
Al_2O_3	0.25	51.0	1.40
Fe_2O_3	0.10	1.9	0.18
MgO	0.03	1.2	2.70
K_2O	0.03	–	–
Na_2O	<0.01	–	–
TiO_2	–	2.6	–
Crystal water	20.10	–	–
Total	98.96	98.7	98.31

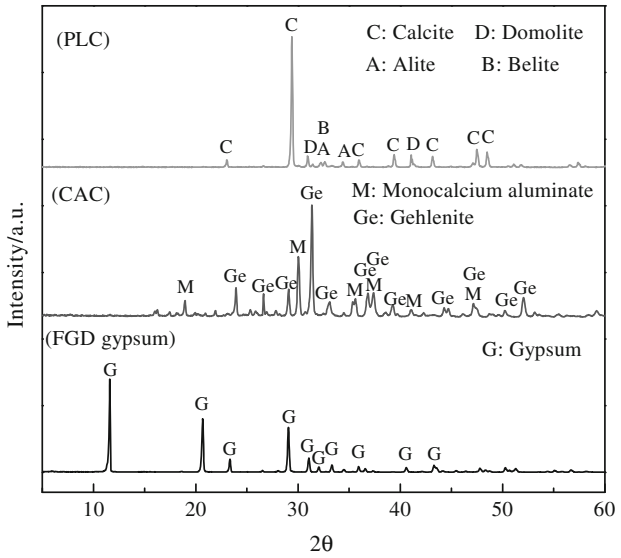

Fig. 1 XRD patterns of FGD gypsum, CAC, and PLC

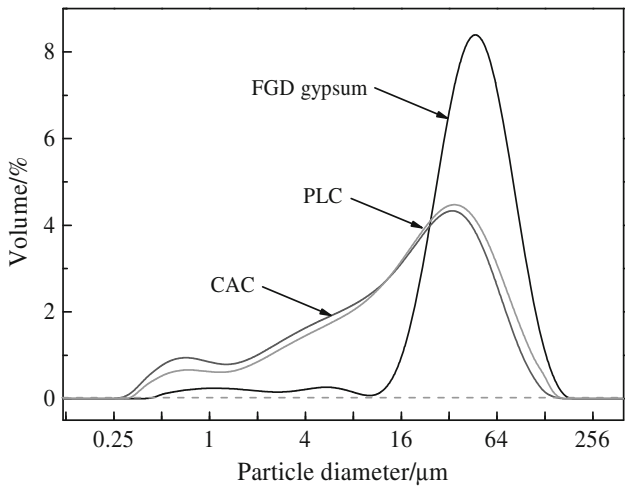

Fig. 2 Particle size distribution of FGD gypsum, CAC, and PLC

and their mean particle sizes are 25.7 and 30.0 μm, respectively.

Preparation of sample and test method

Two groups of binder were designed to investigate the influence of PLC and FGD gypsum on the hydration process and mechanism in the ternary binder of CAC/PLC/FGD gypsum. The FGD gypsum/CAC ratio was set as 0.25 with PLC content from 0 to 40% in group A, while the PLC/CAC ratio was set as 0.25 with FGD gypsum content from 0 to 40% in group B (Table 2). An isothermal heat flow microcalorimeter-TAM Air, manufactured by Thermal Analysis Co. (USA), was employed for calorimetric measurement. Distilled water (2.50 mL) was added into 5.00 g binder giving a water-to-cement mass ratio (w/c) of 0.5, and then the sample was mixed and put into the chamber of calorimeter where it was submerged in an air bath maintained at 20.0 °C.

Pastes were prepared at w/c ratio of 0.35 for setting time determination and XRD analysis. Setting time was measured by using a Vicat test apparatus according to the procedure described in ISO 9597: 1989. At certain hydration time, small pieces of the pastes were soaked in alcohol for 24 h to stop hydration. Then, they were ground in alcohol with an agate mortar and filtrated. The ground samples for XRD analysis were dried in a vacuum oven at 45 °C for 48 h. X-ray diffraction was carried out with RIGAKU D/MAX 2550/PC diffractometer in the range of 5° 2θ–60° 2θ, with step of 0.02°/2 s.

Results

Calorimetric analysis

The curves of heat release rate versus hydration time up to 24 h in the pastes with 0–40% PLC (group A) are illustrated in Fig. 3. In general, the pastes present similar exothermal profiles and vary regularly as the change of compositions.

The exothermal effects associated with wetting, dissolving, and hydrating of components make the appearance of the first exothermal peaks. The pastes with PLC show quite strong exothermal effects in the period, while the paste without PLC shows very slight exothermal effect. After the first exothermal peak, the so-called induction period follows. This period remains about 2.0 h in the paste without PLC, followed by an exothermic peak, where the maximum heat evolution rate is 4.8 mW g^{-1} at 3.8 h. Then, the heat release rate does not drop rapidly but keeps

Table 2 Compositions of ternary binders of CAC/PLC/FGD gypsum

Component	Percentage in binder/wt%													
	A1	A2	A3	A4	A5	A6	A7	B1	B2	B3	B4	B5	B6	B7
CAC	80	76	72	68	64	56	48	80	76	72	68	64	56	48
FGD gypsum	20	19	18	17	16	14	12	0	5	10	15	20	30	40
PLC	0	5	10	15	20	30	40	20	19	18	17	16	14	12

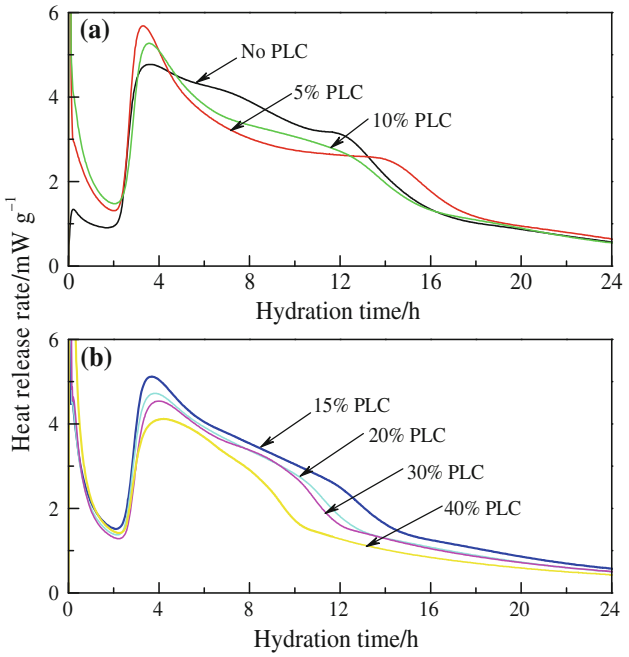

Fig. 3 Heat evolutions of the ternary binders with FGD gypsum/CAC ratio of 0.25 (group A)

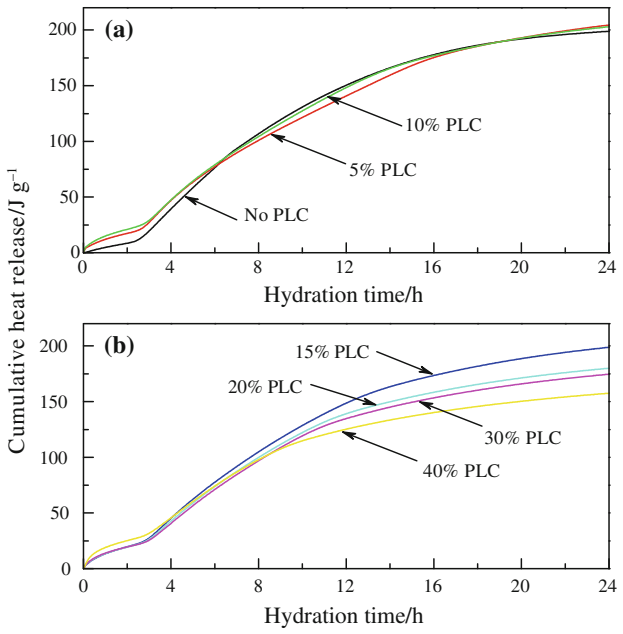

Fig. 4 Cumulative heat evolutions of the ternary binders with FGD gypsum/CAC ratio of 0.25 (group A)

in relative high value, so a 'shoulder' profile is presented. The pastes with PLC also present similar profiles.

The regularity of heat release from the pastes with 5–40% PLC is described as follows: (1) the induction periods are very close and prolong slightly from 2.0 to 2.3 h; (2) the appearances of main exothermal peaks delay from 3.3 to 4.1 h; (3) the maximum rates of heat evolution decline gradually from 5.8 to 4.1 mW g^{-1}; (4) the inflexions in 'shoulder' profiles shorten from 14 to 8 h.

Please note the fact that the maximum heat evolution rates in the pastes with 5–15% PLC are bigger than that of the paste without PLC. It implies that PLC plays an accelerating role in the hydration of such ternary binder.

Plots of cumulative heat evolution up to 24 h in the pastes with 0–40% PLC (group A) are given in Fig. 4. The paste without PLC has the smallest cumulative heat release during the first several hours for its slight exothermal effect of wetting and dissolving period (Fig. 3), and reaches the cumulative heat release of 198.8 J g^{-1} after 24-h hydration. The cumulative heat releases of pastes with 5–40% PLC decline gradually with increase of PLC and their values are 204.4, 202.9, 198.8, 180.0, 174.6, 157.6 J g^{-1}, respectively.

The percentages of total heat released from per gram of binder excluding PLC or limestone, respectively, are shown in Fig. 5. The data are calculated by the results of cumulative heat release in 24 h (Fig. 4). More heat releases from per gram of binder excluding PLC and it shows an ascending profile with increase of PCL (Fig. 5a). So the

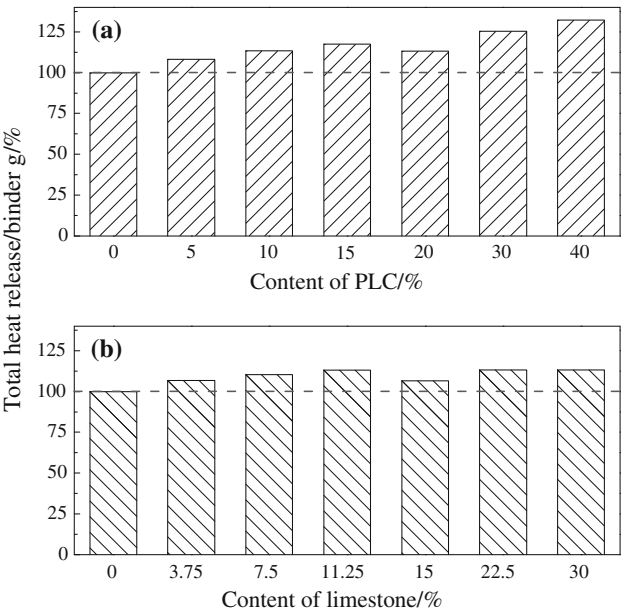

Fig. 5 Comparison of heat release from per gram of binder excluding PLC (**a**) or limestone (**b**)

accelerating effect of PLC on hydration is visualized. The heat release from per gram of binder excluding limestone rises with increase of limestone until 11.25% limestone is blended. It implies that limestone hastens the hydration of binder at certain mass percent but excessive limestone does not affect the hydration anymore. Thus, it is confirmed that the accelerating effect of PLC on hydration in such ternary binder comes from both limestone and PC clinker.

The curves of heat release rate versus hydration time up to 24 h the in pastes with 0–40% FGD gypsum (group B) are illustrated in Fig. 6.

Likewise, the first exothermal peak appears in the initial several minutes, followed by a low heat release period with several hours known as the induction period. The induction period of the paste without FGD gypsum is about 2.2 h followed by a big exothermic peak with the maximum heat release rate of 6.3 mW g^{-1} at around 6.0 h. The induction periods of the pastes with 5–40% FGD gypsum prolong gradually from 2.0 to 2.8 h. A descending of heat release rate with increase of FGD gypsum is found in this period.

Two exothermal peaks besides the first one are observed in the pastes containing 5, 10, and 15% FGD gypsum. The second peaks appear at 3.4, 4.3, and 3.8 h, respectively, and the corresponding heat release rates are 8.1, 5.9, and 5.0 W kg^{-1}. The third peaks appear at 4.3, 6.3, and 9.8 h, respectively, and the corresponding heat release rates are 6.2, 5.2, and 3.8 mW g^{-1}. It presents such tendency that the second peaks appear closely, while the third peaks shift to later ages with the increase of FGD. All pastes with exceeding 15% FGD gypsum present similar heat evolution profiles, that is, the heat release rates decline gradually after their second exothermic peaks. The maximum heat release rates of pastes with 20, 30, and 40% FGD gypsum are 4.8, 4.3, 3.8 mW g^{-1}, respectively, and the corresponding times are at 3.7, 3.9, and 4.2 h.

Figure 7 shows the cumulative heat releases in the pastes with 0–40% FGD gypsum up to 24 h (group B). The

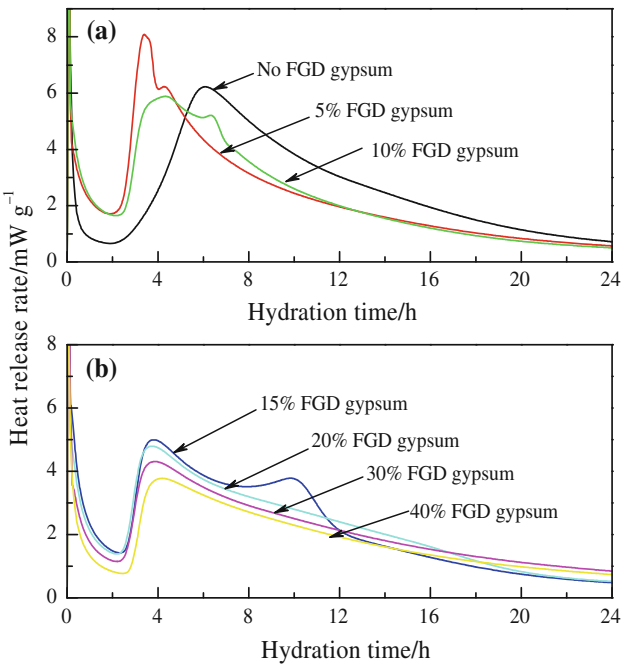

Fig. 6 Heat evolutions of the ternary binders with PLC/CAC ratio of 0.25 (group B)

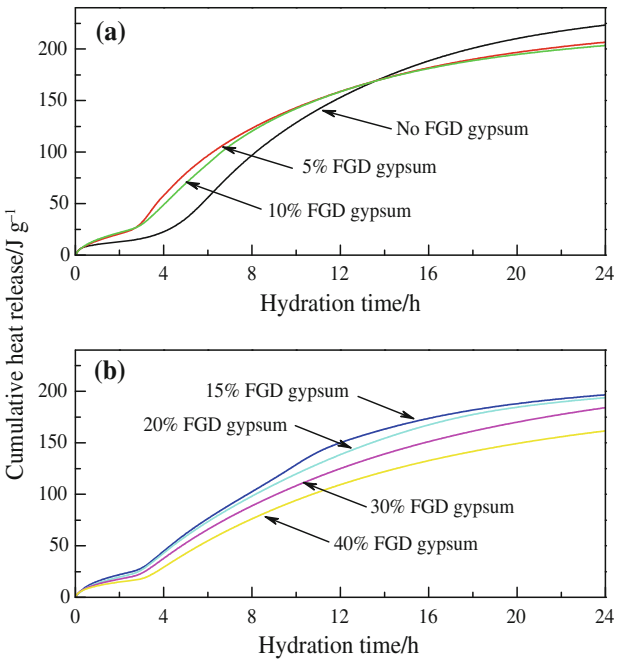

Fig. 7 Cumulative heat evolutions of the ternary binders with PLC/CAC ratio of 0.2 (group B)

pastes with FGD gypsum have bigger cumulative heat release than that of the paste without FGD gypsum in the early age for their stronger exothermal effects during the induction periods (see Fig. 6). After about 14 h, the cumulative heat release of paste without FGD gypsum catches up with those of pastes with FGD gypsum. The paste without FGD gypsum has the biggest cumulative heat release of 223.2 J g^{-1} after 24-h hydration. The cumulative heat releases of pastes with 5–40% FGD gypsum decline gradually from 206.6 to 161.5 J g^{-1}.

The percentages of total heat released from per gram of binder excluding FGD gypsum are shown in Fig. 8. The data are calculated by the results of cumulative heat release in 24 h (Fig. 7). An ascending profile is presented with increase of FGD gypsum, which implies that FGD gypsum generally accelerates the hydration of binder.

Setting times and hydrates analysis

The initial and final setting times of ternary binders are shown in Fig. 9. Setting times of group A do not show remarkable difference varying with PLC content. In general, pastes with 10 and 15% PLC have a little shorter setting times (Fig. 9a). The others have initial setting times of around 120 min and finial setting times of around 175 min. In group B, the pastes without FGD gypsum has the longest initial and final setting time of 190 and 240 min, respectively (Fig. 9b). The initial and final setting times of the pastes with 5–40% FGD gypsum prolong with

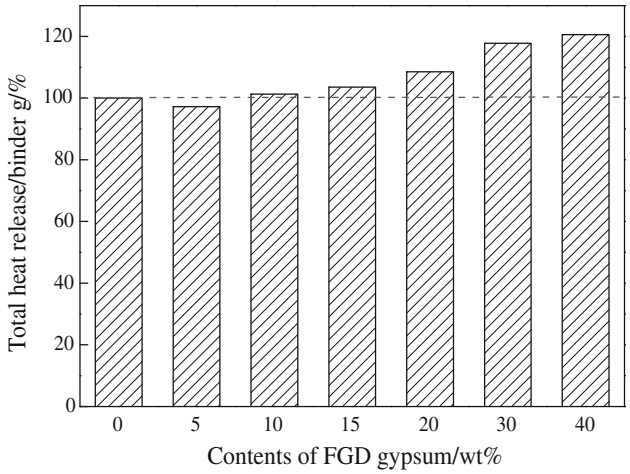

Fig. 8 Heat release from per gram of binder excluding FGD gypsum

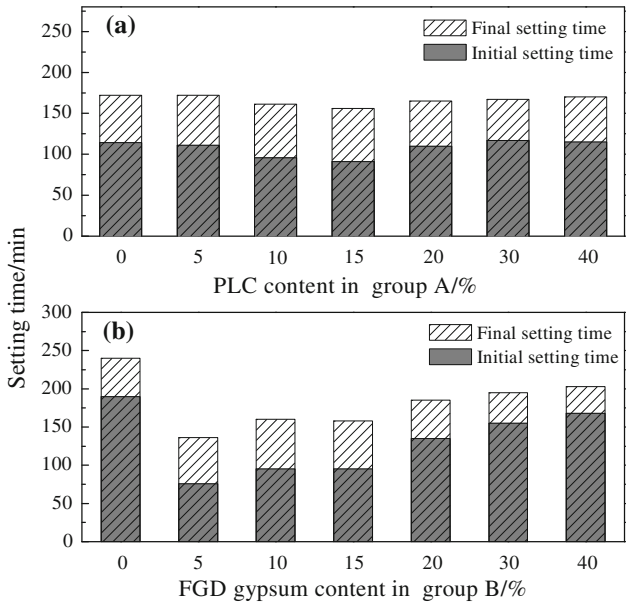

Fig. 9 Setting times of the ternary binders **a** group A, **b** group B)

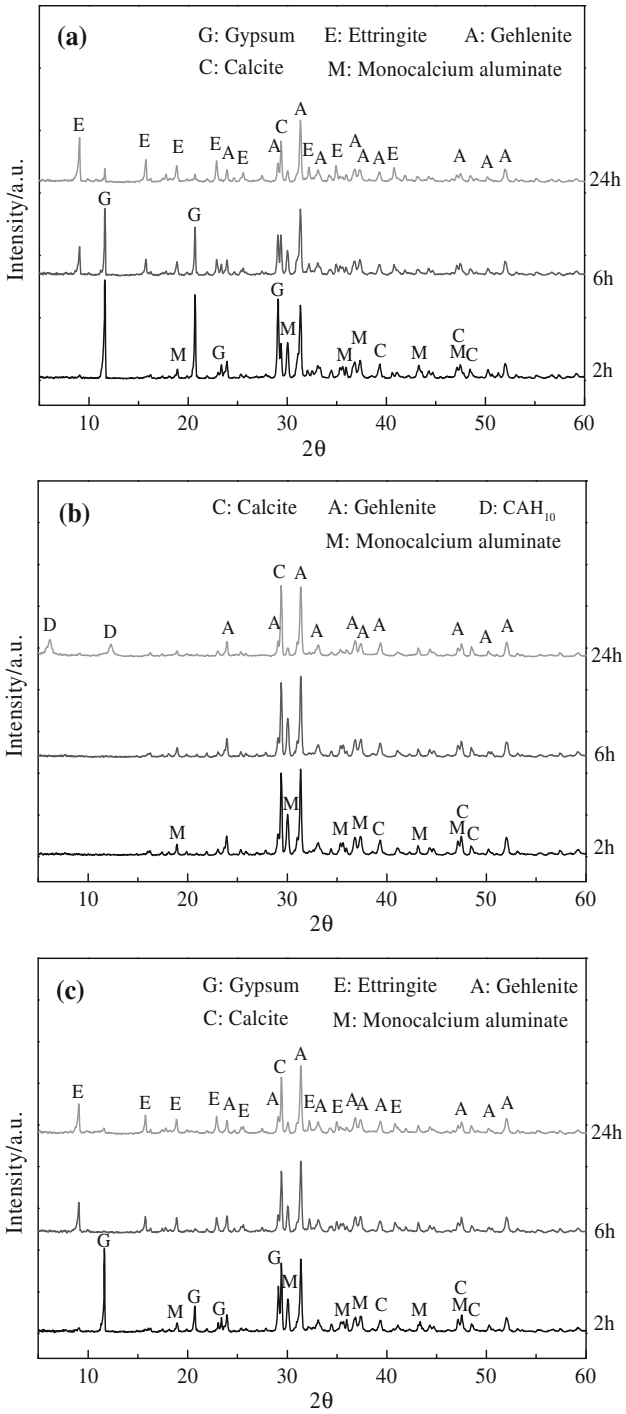

Fig. 10 XRD patterns of the ternary binders at three curing times (2, 6, and 24 h). **a** Paste with 15% PLC, sample A4; **b** paste without FGD gypsum, sample B1; **c** paste with 10% FGD gypsum, sample B3

increase of FGD gypsum, that is the initial setting time prolongs from 75 to 160 min and the final setting time increases from 140 to 210 min.

The XRD patterns of three representative pastes, paste with 15% PLC (sample A4), paste without FGD gypsum (sample B1) and paste with 10% FGD gypsum (sample B3) at three curing times (2, 6, and 24 h) are shown in Fig. 10. The characteristic peaks of main minerals (gehlenite, CA, gypsum, and calcite) in ternary binder are observed in these pastes. The characteristic peaks of C_3S and C_2S can not be clearly determined in these pastes for their low intensity. The peaks of gehlenite and calcite keep nearly the same intensity at different hydration times, while the peak intensities of CA and gypsum decline remarkably as hydration proceeds. After 6-h hydration, gypsum is almost depleted in the paste with 10% FGD gypsum (Fig. 10c), but is still left a little in the paste with 15% PLC, in which 17% FGD gypsum is included (Fig. 10a). The peaks of ettringite appear after the first 2-h hydration in the paste

with FGD gypsum (Fig. 10a, c) and their intensities enhance as hydration goes on. No ettringite but CAH_{10}, the hydrate of CA, is found in the paste without FGD gypsum after 24-h hydration (Fig. 10b). No characteristic peaks of calcium silicate hydrate (C–S–H) are clearly observed.

Discussion

Hydration mechanism of the ternary binder

When the ternary binder is blended with water, the mineral phase of CA, C_3S, and C_2S from cement clinker react with water immediately. The hydration of CA at 20 °C could be described by the following Eq. 3 [26].

$$CA + 10H \rightarrow CAH_{10} \quad (3)$$

Hexagonal phase of CAH_{10} is generated according to this reaction and it is confirmed by XRD analysis (Fig. 10b).

However, when gypsum is mixed, ettringite is directly formed according to Eq. 1 because it has a very low solubility of 1.1×10^{-40} mol L^{-1} [27]. This reaction is certificated by XRD analysis (Fig. 10a, c).

Hydration reactions of C_3S and C_2S can be approximately described by the following chemical equations [28]:

$$2C_3S + 6H \rightarrow 2C{-}S{-}H + 4CH \quad (4)$$

$$2C_2S + 4H \rightarrow 2C{-}S{-}H + 2CH \quad (5)$$

The products formed are a calcium silicate hydrate known as C–S–H and calcium hydroxide (CH). The formula given for C–S–H is only a rough one because more than one variety of C–S–H is formed during the hydration.

Calcium hydroxide mainly comes from the hydration of C_3S and it also may come from the dissolution of free lime, which usually exists in the PC clinker. Thus, the reaction of Eq. 1 is modified by the reaction of Eq. 2 when CH exists.

It is noted that gehlenite peaks keep nearly the same intensity at different hydration time in the pastes (Fig. 10), and this may be attributed to its low hydraulic activity [29, 30]. Theoretically, C_2AS reacts with water as the following Eq. 6:

$$C_2AS + 8H \rightarrow C_2ASH_8 \quad (6)$$

The limestone could be assumed as inert filler and it does not participate the reactions during the first 24-h hydration. An accelerating effect occurs because of the high specific surface of the limestone, and different hydrates can grow on these additional surfaces and thus the dissolution of cement clinker can proceed unhindered leading to a higher degree of hydration [12–15]. This effect is illustrated by Fig. 5b.

As soon as the binder is blended with water, lime and gypsum begin to dissolve, and the hydration of cement clinker occurs simultaneously. Ettringite and other hydrates cover the particles surface of binder. Then, the hydration is inhibited and little heat is released as Figs. 3 and 6 show. Such stage known as induction period can be explained by hypothesis mechanism of hydrate barrier [16, 31]. It supposes that a thin layer of hydration products rapidly covers the entire unhydrated grain when cement reacts with water; a physical barrier impedes further contact between water and the inner cement particles, so the hydration reaction then becomes diffusion controlled. Conformation of the initial hydration layer, which is co-deposited by different hydrate, causes the difference of induction period. The break down of hydrate barrier makes further hydration.

Association of heat release with hydration

The exothermal effect in preliminary minutes of hydration is ascribed to the complex reaction during the wetting process, including the dissolving of lime and gypsum and the hydration of cement clinker (Eqs. 1–5). Then the hydration proceeds in induction period and low heat releases as mentioned above.

With further hydration, large amounts of heat release. The main heat peaks in the pastes (Figs. 3, 6) are believed to result from the reactions of ettringite formation as the hydration mechanism mentioned above. It is clear that the decrease of CAC content makes the gradual decline of the maximum heat lease rate in the pastes with 5–40% PLC (Fig. 3). The heat release 'shoulder' after the main peak is believed mainly comes from the reactions of ettringite precipitation and the hydration of PLC also contributes to this exothermal effect, especially in the pastes with high amount of PLC. The shortening of inflexions in 'shoulder' profiles may contribute to the decrease of CAC content (Fig. 3).

The accelerating effect of PLC on hydration is clearly visualized by the calorimetric analysis: (1) the maximum heat evolution rates in the pastes with 5–15% PLC are bigger than that of the paste without PLC (Fig. 3); (2) the heat release from per gram of binder excluding PLC rises with increase of PLC (Fig. 5a). Limestone accelerating hydration is also well-illustrated (Fig. 5b). However, excessive limestone does not accelerate the hydration anymore when enough additional surfaces are supplied by limestone according to the nucleating mechanism [12–15]. As PC is concerned in the hydration of binder, the hydrate of CH modifies the hydration mechanism (Eq. 2) results in more heat release because ettringite has a big synthetic heat. Besides, the PC clinker could also supply additional surfaces as limestone for precipitation of hydrates from CAC clinker. The two coexisting mechanisms make PC put a complicated effect on the hydration of binder.

The calorimetric profile of the paste without FGD gypsum in group B is controlled by the hydration of CAC and

PLC (Fig. 6), which hydration mechanism is well revealed by the hydrate barrier mechanism [16]. The second exothermic peak in the pastes with 5, 10, and 15% FGD gypsum is obviously attributed to the reaction of ettringite formation and the third one is clearly connected with the hydration of CAC when FGD gypsum is depleted. This is approved by XRD analysis in Fig. 10c, where gypsum is depleted after 6-h hydration. The depletion of FGD gypsum takes much more time when FGD gypsum increases from 5 to 15% in the pastes, which makes the third exothermal peak shift to later hydration time with increase of FGD gypsum (Fig. 6). The whole hydration process is controlled by the reaction of ettringite formation in the pastes with exceeding 15% FGD gypsum, so the third exothermal peak does not appear (Fig. 6). The decline of the maximum heat release rate with the increase FGD gypsum is obviously attributed to the decrement of CAC or the dilution effect of excessive FGD gypsum. In fact, such exothermal profiles in the pastes of group B are quite similar with those of CAC blended with FGD gypsum in our previous work [25]. The difference is that the exothermic effect during the first heat release peak and induction period is stronger than that of binary binder. In this case, the accelerating effect of PLC on hydration is also illustrated.

It is concluded that PLC does not play the crucial role in such ternary binder where the reaction of ettringite formation dominates the hydration process from both results of group A and B.

Association of setting time with hydration

Setting occurs when enough hydrates have formed to interlock particles and restrict their flow. Setting time is intrinsic reflections of the hydrating processes and the matrix structure formations in the pastes. As hypothesis mechanism of hydrate barrier, the paste does not set until the breakdown of this barrier by nucleation of ettringite and other hydrates. The initial setting times of the pastes coincide well with the heat release regulation, that is, the initial setting time is close with the ending of induction time for each paste (Figs. 3, 6). The quick setting of pastes in both group A and B is beneficial for early strength development, and it is favorable in some building construction such as self-leveling floor screed.

Conclusions

Based on the experiment results, it could be concluded that:

- The reaction of ettringite formation dominates the whole hydration process in all pastes of group A, and the same hydration mechanism brings out regular heat lease.
- The reaction of ettringite formation and CAC hydration control the hydration process successively in the pastes with 5–15% FGD gypsum (group B). The modified hydration mechanism makes different heat lease, that is, a third exothermal peak appears when FGD gypsum is depleted. It indicates the FGD gypsum content has a significant influence on the hydration behavior.
- PLC accelerates the hydration of such ternary binder, which is mainly due to the nucleating effect of fine particles from limestone and PC clinker. For the same reason, excessive limestone does not accelerate the hydration when the content is over 11.25%, because enough additional surfaces have been supplied.
- CH, the hydrate of C_3S and C_2S modifies the hydration mechanism to form more ettringite. Thus, more FGD gypsum could be blended in the ternary binder with increase of PC clinker.

Acknowledgements The authors acknowledge greatly the financial support of this work by the fund of Chinese National Program for High Technology Research and Development (Project No. 2006AA03Z385), Science and Technology Plan of Zhejiang Province, China (Project No. 2007C23055) and the New Century 151 Talent Project of Zhejiang Province.

References

1. Hamm H, Kersten HJ, Hueller R. 25 years experience gained in the European Gypsum Industry with the use of FGD gypsum. Cem Int. 2004;4:92–102.
2. Guo XL, Shi HS. Thermal treatment and utilization of flue gas desulphurization gypsum as an admixture in the cement and concrete. Constr Build Mater. 2008;22:1471–6.
3. Tzouvalasl G, Rantis G, Tsimas S. Alternative calcium-sulfate-bearing materials as cement retarders: Part II. FGD gypsum. Cem Concr Res. 2004;34:2119–25.
4. Glasser FP, Zhang L. High-performance cement matrices based on calcium sulfoaluminate-belite compositions. Cem Concr Res. 2001;31:1881–6.
5. Péra J, Ambroise J. New applications of calcium sulfoaluminate cement. Cem Concr Res. 2004;34:671–6.
6. Glasser FP, Zhang L, Zhou Q. Reactions of aluminate cements with calcium sulphate. In: Proceedings of international conference on calcium aluminate cements (CAC), Heriot-Watt University, Edinburgh, Scotland, 2001, pp. 551–64.
7. Deng M, Tang M. Formation and expansion of ettringite crystals. Cem Concr Res. 1994;24:119–26.
8. Adams LD. Ettringite, the positive side. In: Proceedings of the 19th international conference on cement microscopy, Cincinnati, Ohio, ICMA, Duncanville, TX, 1997, pp. 1–13.
9. Amathieu L, Estienne F. Impact of the conditions of ettringite formation on the performance of products based on CAC+C-S+OPC. Weimar: 15. Internationale Baustofftagung; 2003. pp. 1-0253–63.
10. European Committee for Standardization. Cement: composition, specifications and conformity Criteria, Part 1: common Cements, EN 197-1, EN/TC51/WG 6 rev., 2000.
11. Lothenbach B, Saout GL, Gallucci E, Scrivener K. Influence of limestone on the hydration of Portland cements. Cem Concr Res. 2008;38:848–60.

12. Poppe AM, Schutter GD. Cement hydration in the presence of high filler contents. Cem Concr Res. 2005;35:2290–9.
13. Dweck J, Buchler PM, Coelho ACV, Cartledge K. Hydration of a Portland cement blended with calcium carbonate. Thermochim Acta. 2000;346:105–13.
14. Kuzel HJ, Baier H. Hydration of calcium aluminate cements in the presence of calcium carbonate. Eur J Mineral. 1996;8:129–41.
15. Darweesh HHM. Limestone as an accelerator and filler in limestone-substituted alumina cement. Ceram Int. 2004;30:145–50.
16. Gu P, Beaudoin JJ. A conduction calorimetric study of early hydration of ordinary Portland cement/high alumina cement pastes. J Mater Sci. 1997;32:3875–81.
17. Evju C. Initial hydration of cementitious systems using a simple isothermal calorimeter and dynamic correction. J Therm Anal Calorim. 2003;71:829–40.
18. Pacewska B, Blonkowski G, Wilińska I. Investigations of the influence of different fly ashes on cement hydration. J Therm Anal Calorim. 2006;86:179–86.
19. Baert G, Hoste S, De Schutter G, De Belie N. Reactivity of fly ash in cement paste studied by means of thermagravimetry and isothermal calorimetry. J Therm Anal Calorim. 2008;94:485–92.
20. Rahhal V, Cabrera O, Talero R, Delgado A. Calorimetry of portland cement with silica fume and gypsum additions. J Therm Anal Calorim. 2007;87:331–6.
21. Rahhal V, Talero R. Calorimetry of Portland cement with metakaolins, quartz and gypsum additions. J Therm Anal Calorim. 2008;91:825–34.
22. Roszczynialski W, Nocuń-Wczelik W. Studies of cementitious systems with new generation by-products from fluidized bed combustion. J Therm Anal Calorim. 2004;77:151–8.
23. Sawków J, Nocuń-Wczelik W. Calorimetric studies of refractory corundum calcium aluminate composites. J Therm Anal Calorim. 2003;74:451–8.
24. Gawlicki M, Nocuń-Wczelik W, Bąk Ł. Calorimetry in the studies of cement hydration. J Therm Anal Calorim. 2009. doi: 10.1007/s10973-009-0158-5.
25. Guan B, Lou W, Ye Q, Fu H, Wu Z, Calorimetric study of calcium aluminate cement blended with flue gas desulfurization gypsum. J Therm Anal Calorim. 2009. doi:10.1007/s10973-009-0107-3.
26. Scrivener KL. High-performance concretes from calcium aluminate cement. Cem Concr Res. 1999;29:1215–23.
27. Gu P, Fu Y, Xie P, Beaudoin JJ. A study of the hydration and setting behavior of OPC-HAC paste. Cem Concr Res. 1994;24:682–94.
28. Taylor HFW. Cement chemistry. 2nd ed. London: Thomas Telford; 1997.
29. Smrčková E, Palou M, Tomková V. Application of conduction calorimetry for study of the reactivity of C2S–C4A3Ŝ–CŜ–H. J Thermal Anal. 1996;46:597–605.
30. El-Didamony H, Khalil KA, El-Atter MS. Physicochemical characteristics of fired clay-limestone mixes. Cem Concr Res. 2000;30:7–11.
31. Regourd M, Thomassion JH, Baillif P, Touray JC. Study of the early hydration of Ca_3SiO_5 by X-ray photoelectron spectrometry. Cem Concr Res. 1980;10:223–30.